Valence band and Sb 4d core level photoemission of the XMnSb-type Heusler compounds (X=Pt,Pd,Ni)

1995 J. Phys.: Condens. Matter 7 3789

(http://iopscience.iop.org/0953-8984/7/19/013)

J. Phys.: Condens. Matter 7 (1995) 3789–3800. Printed in the UK

Valence band and Sb 4d core level photoemission of the XMnSb-type Heusler compounds (X = Pt, Pd, Ni)

J-S Kang†, J-G Park‡*, C G Olson§, S J Youn¶ and B I Min¶

† Research Institute of Industrial Science and Technology, Pohang 790-600, Korea

‡ *Department of Physics, Imperial College, London SW7 2BZ, UK*

§ Ames Laboratory, Iowa State University, Ames, Iowa 50011, USA

¶ Department of Physics, Pohang University of Science and Technology, Pohang 790-784, Korea

Received 23 January 1995, in final form 21 March 1995

Abstract. Electronic structures of the valence band and Sb 4d core levels of the XMnSb-type Heusler alloys (where X = Pt, Pd, Ni) have been investigated systematically using photoemission spectroscopy (PES) and self-consistent spin-polarized band structure calculations. The extracted Mn 3d PSW of XMnSb (where X = Pt, Pd) are found to be almost identical. Interestingly, they are quite different from those of Mn metal, but are analogous to those of MnO, suggesting that the role of the Sb 5p electrons in XMnSb may be similar to that of the O 2p electrons in MnO. A comparison of the PSW with the corresponding theoretical angular momentum projected density of states (PLDOS) shows a fairly good agreement for the Pt and Pd d states, but large discrepancies for the Mn and Ni 3d states. The calculated X d and Mn 3d PLDOS reveal that the hybridization between the Mn 3d and X d states increases from X = Pt to Pd and Ni. In the Sb 4d core level PES spectra, a broader and less structureless line shape is observed for X = Pd than for X = Pt and Ni. A detailed analysis of their line shapes indicates that it is due to a larger lifetime broadening for X = Pd than for X = Pt and Ni.

1. Introduction

Mn-based Heusler alloys of the formula XMnSb, with X = Pt, Pd, Ni, belong to an interesting class of magnetic metals. These compounds are strong ferromagnets with high Curie temperatures T_C [1]. Band structure calculations for PtMnSb and NiMnSb [2–7] show that the majority-spin electrons are metallic while the minority-spin electrons are semiconducting. As a consequence, the conduction electrons at the Fermi level E_F are 100% spin polarized. PtMnSb exhibits the largest magneto-optical Kerr effect (MOKE) at room temperature among the known metallic systems [1, 8]. A large MOKE in a half-metallic compound is considered to be closely related to its electronic structure, which gives rise to incomplete cancellations of left- and right-polarized electronic excitations [4, 5, 9].

A first test of the half-metallic character of NiMnSb has been performed by Bona and co-workers [10] by spin-resolved photothreshold emission, in which the observed spin polarization was only about 50%, in contrast to the expected 100% spin polarization near the threshold. Kisker and co-workers [11] reported preliminary studies on PtMnSb(100) by using spin-averaged and angle-resolved photoelectron spectroscopy (PES), and concluded that the agreement between experimental and theoretical band structures is very good. However, their data were preliminary, as the authors admitted, and so the experimental results need to

* Present address: Department of Physics, Birkbeck College, University of London, London WCIE 7HX, UK.

0953-8984/95/193789+12$19.50

be re-confirmed. Robey and co-workers [12] have performed resonant photoemission (RPES) investigations on Ni_2MnSb and NiMnSb, and compared the PES data with the calculated density of states (DOS). They concluded that the experimental and theoretical band structures reveal reasonable agreement, although the calculations overemphasize the contribution of the Ni 3d states at some binding energies. However, the quality of the PES data by Robey and co-workers was not so good†. Kang and co-workers [13] have previously reported PES results on PtMnSb and NiMnSb, in which they extracted the Mn 3d partial spectral weight (PSW) of PtMnSb. They found that the hybridization between the Mn 3d and other conduction electrons is large, and that there are substantial discrepancies between the measured PES spectra and the calculated band structure predictions. Recently Yang and co-workers [14] have studied the Mn 2p and 3s core level spectra of XMnSb (X = Pt, Pd, Ni) using x-ray photoelectron spectroscopy (XPS). They observed large intensities of Mn 2p satellites and exchange split 3s satellites, as compared to other metallic Mn alloys, which were considered to indicate the atomic character of the host Mn atoms and localization of d electrons at the Mn site.

As summarized above, there are several issues to be resolved in the electronic structures of the XMnSb–type Heusler alloys (X = Pt, Pd, Ni). First, in spite of extensive theoretical works which consistently predict the half-metallic character of XMnSb (X = Pt, Ni), experimental investigations on their electronic structures have only partially succeeded in identifying the half-metallic character of these Heusler alloys. Second, the role of X atoms (X = Pt, Pd, Ni) in their electronic structures is not yet clarified. It is generally suggested that X atoms serve primarily to determine the lattice constant and the Sb atom mediates the interaction between Mn 3d states [6], implying the importance of the hybridization between Mn 3d and Sb 5p electrons. However, there has been no experimental confirmation of this suggestion as yet. Third, the origin of their ferromagnetic properties is not well understood. Neutron diffraction measurements [1, 15] showed that the magnetic moments are confined to the Mn atoms, consistent with the band structure predictions. However, distances between Mn atoms are too large for direct exchange interactions.

In order to deduce a systematic trend in XMnSb as X varies from a 5d to 4d transition metal element, we extend in this paper previous valence band PES investigations of XMnSb from X = Pt, Ni to X = Pt, Pd, Ni. Note that according to band structure calculations [2, 16] PdMnSb is just a normal metal in contrast to PtMnSb and NiMnSb. New information and the advantages of the present work are as follows. (i) Our PES data are obtained from the surfaces free from oxygen (O) and carbon (C) contamination, and so the data are very reliable (see section 2). (ii) Using the photon energy $h\nu$ dependence of the photoionization cross sections, the PSW of the Mn 3d, Pt 5d and Pd 4d valence electrons are extracted for XMnSb (X = Pt, Pd). (iii) A systematic and detailed comparison is made between PES data and theoretical results for XMnSb (X = Pt, Pd, Ni). (iv) Studies of the Sb 4d core levels are included, which provide indirect information on the valence electronic structure of the Sb 5p electrons. This will complement the XPS studies of Mn 2p and 3s core levels by Yang and co-workers [14].

2. Experimental details and calculational methods

The samples were made by melting carefully weighed constituent elements encapsulated in a vacuum-sealed quartz tube at 1100 °C; about 5% of weight loss was observed during

† By comparing the data for NiMnSb in figure 7 of [12] with those in figure 1(*b*) of [13], one can clearly see that the data by Robey and co-workers do not exhibit several features which were observed in [13], and that the quality of their data is not so good.

the melting process. Subsequently the samples underwent a proper annealing procedure at 600 °C for one week. X-ray diffraction (XRD) measurements indicated that most of the samples were crystallized in a single-phase cubic structure of MgAgAs type [17], with an impurity phase less than 5% in PtMnSb; electron-probe analysis using scanning electron microscopy (SEM) identified this impurity phase to be an *Mn-depleted* phase.

Photoemission measurements were performed at the Synchrotron Radiation Center of the University of Wisconsin-Madison, on the Mark V beam line. The polycrystalline samples were cleaved *in situ* and measured at ~ 60 K in a vacuum better than 4×10^{-11} Torr. No O or C contamination was detected in the valence band spectra, taken at low $h\nu$, as well as in the C 1s core level spectra†. The overall instrumental resolution of the system (full width at half maximum FWHM) is ~ 0.2 eV at $h\nu = 40$ eV and ~ 0.4 eV at $h\nu = 150$ eV, respectively. The photon flux was monitored by the yield from a gold mesh and all the spectra reported in this paper were normalized to the incident photon flux.

The angular momentum projected local density of states (PLDOS) is obtained [7] from the self-consistent LMTO (linear muffin-tin orbital) spin-polarized band structure calculations [18] using the local density functional approximation (LDA) [19]. The effect of the spin–orbit interaction is explicitly included. In obtaining the density of states, Brillouin zone integration is done using the tetrahedron method. Our LMTO band calculations, by including the spin–orbit interactions, yield that NiMnSb and PtMnSb are half-metallic at the experimental lattice constants, while PdMnSb is a normal metal at the experimental lattice constant. The details of calculations are described in [7].

3. Results and discussion

3.1. PSW and PLDOS of valence band electrons

Figure 1 shows valence band energy distribution curves (EDC) of PdMnSb. The range of $h\nu$ includes the 3p $\rightarrow$ 3d absorption thresholds of Mn and Ni and the Cooper minimum of the Pd 4d cross section [20]. A broad peak at a binding energy (BE) around 10 eV for $h\nu = 52$ eV is due to Mn MVV Auger emissions. At $h\nu \sim 40$ eV, the Pd 4d electron emissions are dominant over other electron emissions [21]. As $h\nu$ increases, the fraction of the Mn 3d emission increases, and becomes dominant near the Cooper minimum in the Pd 4d photoionization cross section ($h\nu \sim 120$ eV)‡. Hence the spectra near the Cooper minima can be considered to represent the Mn 3d PSW of PdMnSb. The inset compares the valence band spectrum of PdMnSb (full curves), taken at $h\nu = 120$ eV, with that of PtMnSb (dots), taken at $h\nu = 150$ eV, which corresponds to the Cooper minimum in the Pt 5d photoionization cross section. In both spectra, inelastic backgrounds have been subtracted by using a standard method [22].

Figure 1 reveals several interesting features in the Mn 3d electronic structures. First, the Mn 3d PSW of PdMnSb is very similar to that of PtMnSb, as shown in the inset. This indicates that the overall features of the Mn 3d electronic structure are insensitive to X in

† In these compounds, the O 1s binding energy overlaps with the Sb 3d binding energies, and so direct observation of the O 1s core levels is obscured. However, the line shapes of the Sb 3d core levels, as well as those of Sb 4d core levels (see figure 7), suggest that all the measured surfaces are free of oxygen contamination.

‡ According to atomic photoionization cross sections, the Mn 3d emission with respect to the Pt 5d or Pd 4d emissions will be about 25% at $h\nu \sim 40$ eV, whereas the Pt 5d or Pd 4d emissions with respect to the Mn 3d emission will be only about 10% at $h\nu \sim 150$ eV in PtMnSb and at $h\nu \sim 120$ eV in PdMnSb, respectively. The total contribution from other electrons, such as Sb 5s/5p, Mn 4s, Pt 6s and Pd 5s electrons, are always less than 10% with respect to that from Mn 3d, Pt 5d or Pd 4d electrons.

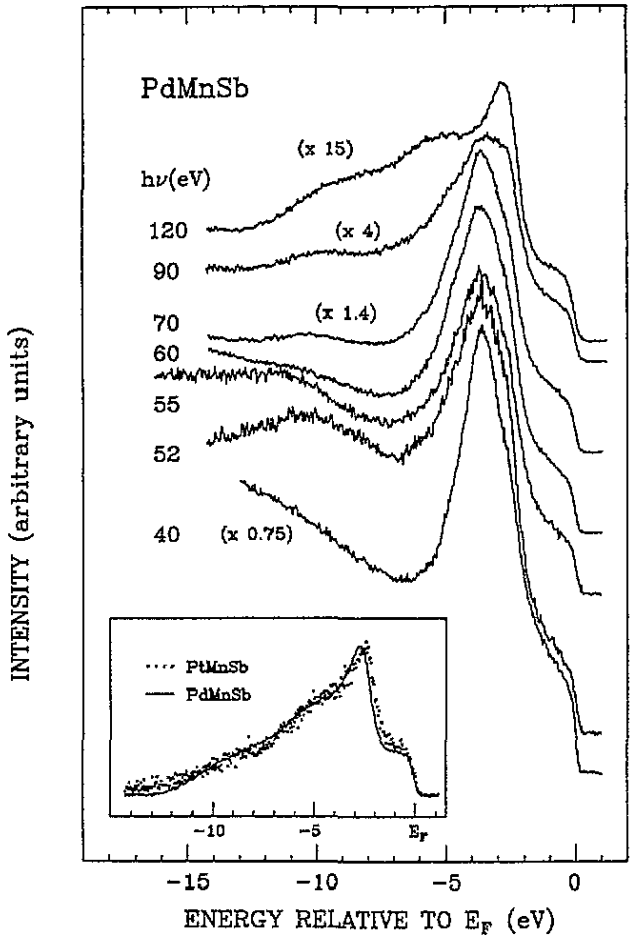

Figure 1. Valence band energy distribution curves (EDC) of PdMnSb, for different photon energies ($h\nu$). Inset: comparison of the valence band EDC of PdMnSb at $h\nu = 120$ eV (full curves) with that of PtMnSb at $h\nu = 150$ eV (dots).

XMnSb for X = Pt and Pd. Second, the Mn 3d emission extends over the entire valence band from E_F down to −10 eV, suggesting large hybridization between Mn 3d and other valence electrons. Third, in spite of the metallic character of PtMnSb and PdMnSb, their Mn 3d PSW are quite different from that of Mn metal [23, 24], but are very similar to that of MnO [25–27], which is an insulating compound. This suggests that the role of the Sb 5p electrons in XMnSb might be similar to that of the O 2p electrons in MnO in determining the Mn 3d electronic structures. Based on this observation, it is tempting to assume that the magnetic exchange interaction in XMnSb might be attributed to the superexchange interaction, as in MnO [28]. However, superexchange exists only in magnetic insulators, and so the mechanism for the magnetic interaction in XMnSb will not be exactly the same as that in MnO.

Figures 2(*a*) and (*b*) compare the experimental PSW (dots) with the calculated PLDOS (full curves) for Mn 3d and Pt 5d states for PtMnSb, respectively. For comparison with other compounds, figure 2(*b*) is reproduced from [13]. The Mn 3d PSW is the spectrum taken at $h\nu = 150$ eV, and the Pt 5d PSW corresponds to the difference between the 60 eV

and 150 eV spectra by taking into account the $h\nu$ dependence of the photoionization cross sections of the valence electrons [21]. Inelastic backgrounds have been subtracted from the measured spectra [22]. To compare with the experimental PSW below E_F, the calculated majority- and minority-spin PLDOS are summed and only the occupied parts of the results are presented. Calculated PLDOS have been convolved with a Gaussian of 0.4 eV at FWHM to simulate the instrumental broadening.

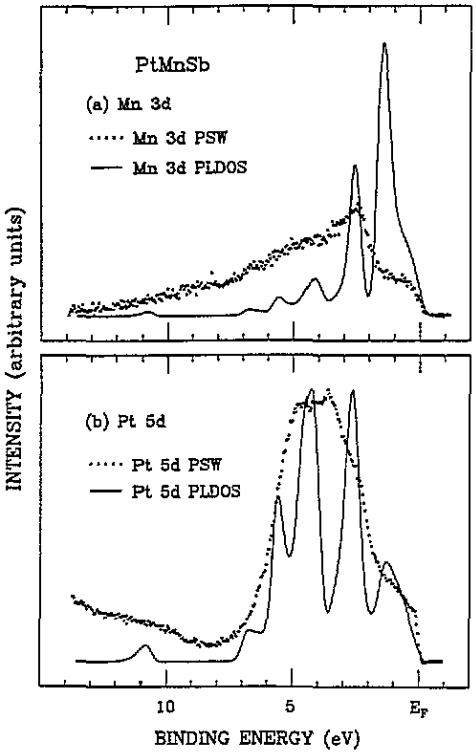

Figure 2. (*a*) Comparison of the Mn 3d partial spectral weight (PSW) with the calculated Mn 3d angular momentum projected local density of states (PLDOS) in PtMnSb. (*b*) Same for Pt 5d states in PtMnSb.

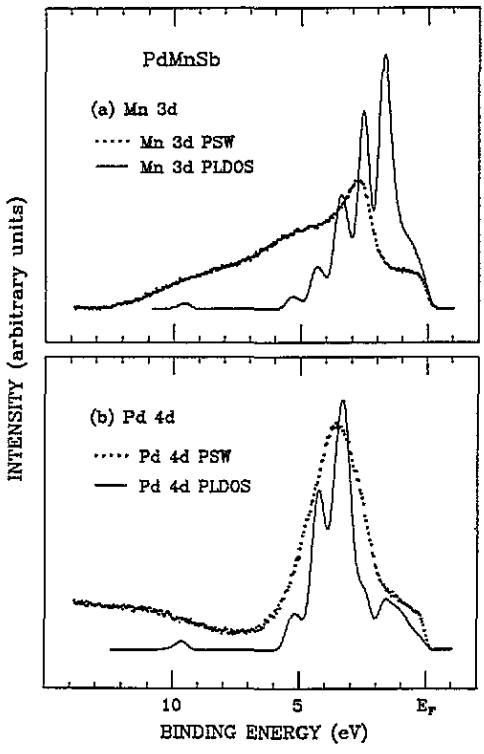

Figure 3. (*a*) Comparison of the Mn 3d PSW with the Mn 3d PLDOS in PdMnSb. (*b*) Same for Pd 4d states in PdMnSb.

The calculated Mn 3d PLDOS predicts the experimental Mn 3d character at -3 eV rather well. However, it fails to describe the experimental Mn 3d spectral weight between -10 eV and -6 eV, and the predicted strong peak at ~ 1.5 eV is not observed in experiment. These discrepancies between theory and experiment may be partially due to the effects of a finite lifetime of a valence hole, photoionization matrix elements and relaxation in photoemission process, which are not included in the theoretical curves. But the major contribution to the disagreement seems to be due to the large Coulomb correlation among Mn 3d electrons. The semiconducting character of Mn 3d minority-spin bands might also cause such discrepancies, as the LDA does not describe a semiconducting behaviour very well. On the other hand, the calculated Pt 5d PLDOS and the experimental Pt 5d PSW in PtMnSb agree with each other reasonably well in band widths and peak positions.

Similarly as in PtMnSb, the experimental PSW and the calculated PLDOS of Mn 3d and Pd 4d states of PdMnSb are compared in figures 3(*a*) and (*b*), respectively. The findings in

PdMnSb are similar to those in PtMnSb, in that Mn 3d states exhibit a large disagreement while Pd 4d states exhibit a fairly good agreement between experiment and theory. Note that the Pt 5d PSW in figure 2(*b*) and Pd 4d PSW in figure 3(*b*) share some features which exhibit systematic trends: (i) the FWHM of X d PSW in XMnSb decreases from X = Pt to X = Pd (~ 4 eV in PtMnSb and ~ 3 eV in PdMnSb), and (ii) the weight centre of the X d PSW shifts toward E_F as X varies from Pt (at ~ −4 eV) to Pd (at ~ −3.5 eV). These two trends of X d PSW are consistent with those of the calculated X d PLDOS (X = Pt, Pd), which will be presented in figure 6.

For NiMnSb, it is difficult to extract either the Ni 3d PSW or the Mn 3d PSW for the following reasons. First, Ni and Mn 3d photoionization cross sections are of comparable magnitudes at most photon energies†. Second, the effects of the resonance in the Ni and Mn 3d cross sections near the 3p → 3d absorption edges [12, 13], are not large enough for the Ni or Mn 3d PSW to be extracted. Therefore, we compare the spectrum of $h\nu = 130$ eV with the weighted sum of Ni and Mn 3d PLDOS in figure 4, in which the Mn 3d and Ni 3d PLDOS are multiplied by the factors 1:2, respectively, to take into account the photoionization cross sections.

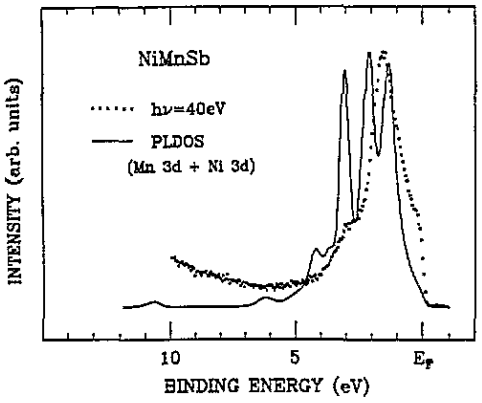

Figure 4. Comparison of the valence band EDC at $h\nu = 130$ eV with the weighted sum of the Mn 3d and Ni 3d PLDOS in NiMnSb. For details, refer to the text.

In figure 4, a broad emission between −10 and −5 eV in the measured spectrum is considered to be a mixture of the Ni 3d satellite structure [13] and the tail of the Mn 3d PSW as in PtMnSb and PdMnSb. First, this figure shows that the calculated PLDOS near E_F is very small due to the predicted half-metallic character of NiMnSb, whereas the measured spectral weight near E_F is much larger than the calculated PLDOS near E_F. Second, the FWHM of the calculated PLDOS is larger than that of the PES spectrum by ~ 1 eV. Finally, the major PLDOS peaks are located farther from E_F than the PES peaks by more than 0.5 eV. We believe that these discrepancies between experiment and theory reflect large *on-site* Coulomb interactions among the Mn 3d and Ni 3d electrons. This argument will be supported by the reasons given below.

† Ni and Mn 3d emissions in NiMnSb are not only comparable with each other, but also much larger than other electron emissions for 40 eV < $h\nu$ < 90 eV. This is indeed observed experimentally in the way that the measured PES line shapes are rather insensitive to a variation in $h\nu$ (see [13]). The photoionization cross section of the Mn 3d electrons is comparable to that of the Ni 3d electrons near $h\nu = 40$ eV, decreases with increasing $h\nu$, and becomes about half of the latter near $h\nu = 130$ eV.

In order to identify the systematic trends in the X and Mn d electronic structures of XMnSb (X = Pt, Pd, Ni), we have compared the calculated Mn 3d and X d PLDOS in figures 5 and 6, respectively. Full curves represent the summation of the majority- and minority-spin PLDOS, and broken curves represent the majority-spin PLDOS only. In figure 5, the Mn 3d PLDOS below and above E_F are mainly due to the majority and minority spin bands, respectively, in all compounds. The separation between the main peaks in the majority-spin states and those in the minority-spin states, which can be a rough measure of Mn 3d exchange splittings, decreases as X varies from Pt to Pd and Ni. This trend is consistent with the calculated magnetic moment at the Mn site in XMnSb, which decreases as X varies from Pt to Pd and Ni [7].

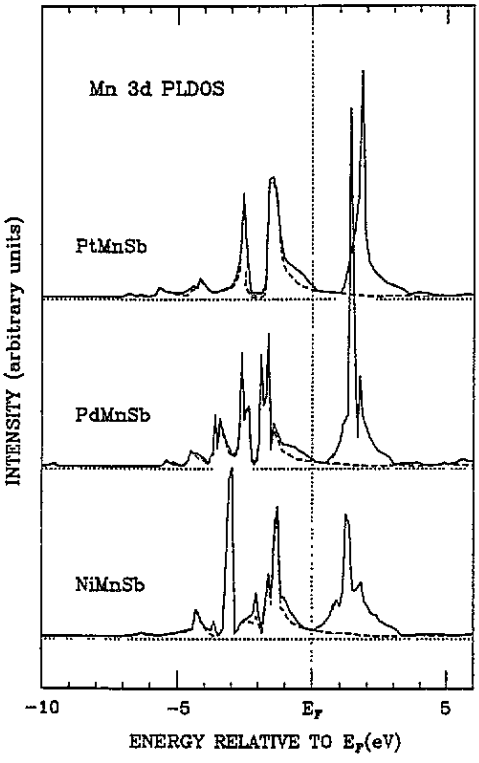

Figure 5. Comparison of the Mn 3d PLDOS in XMnSb (X = Pt, Pd, Ni). Full curves represent the summation of the Mn 3d majority- and minority-spin PLDOS. Broken curves represent the majority-spin Mn 3d PLDOS only.

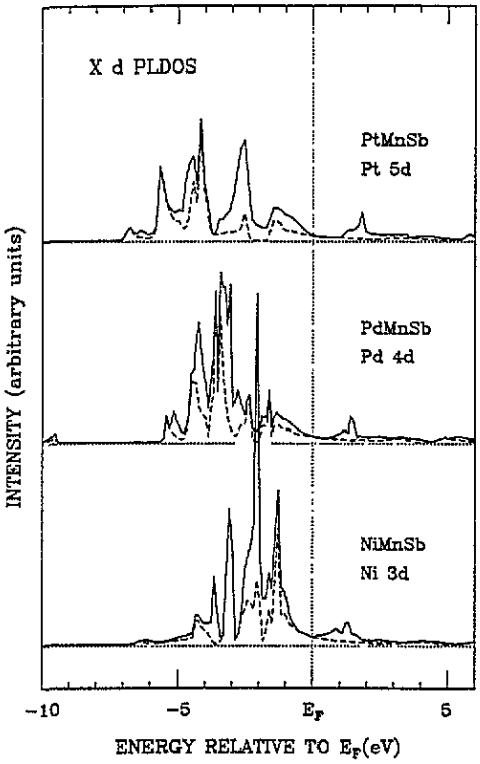

Figure 6. Comparison of the X d PLDOS in XMnSb (X = Pt, Pd, Ni). Full curves represent the summation of the X d majority- and minority-spin PLDOS. Broken curves represent the majority-spin PLDOS only.

Figure 6 compares the calculated X d PLDOS of XMnSb (X = Pt, Pd, Ni). In all three compounds, the small peaks above E_F are due to minority-spin states. Note that the occupied band width of the X d PLDOS decreases from X = Pt to Pd and Ni, suggesting that the Coulomb correlation effect among X d electrons increases from X = Pt to Pd and Ni. This phenomenon provides an explanation of why good agreement was observed between the experimental PES band width and the calculated PLDOS width for Pt 5d states, while poor agreement was observed for Mn and Ni 3d states in XMnSb (see figures 2–4). For X = Pt, the weight centre of the majority-spin states is well below E_F. In contrast, for X = Ni, the weight centre of the majority-spin states is located closer to E_F. In consequence, the Pt 5d

majority-spin states hardly overlap with the Mn 3d majority-spin states in PtMnSb, while the Ni 3d majority-spin states overlap substantially with the Mn 3d majority-spin states in NiMnSb.

The more the X d states overlap with the Mn 3d states in XMnSb, the larger the hybridization interaction between the Mn 3d and X d states. The increasing hybridization between the Mn 3d and X d states from X = Pt to Pd and Ni would cause a decreasing magnetic moment per Mn atom from X = Pt to Pd and Ni. On the other hand, a larger hybridization would give rise to a larger T_C. This is because the hybridization interaction between the Mn 3d and X d states induces an indirect magnetic exchange interaction between Mn atoms, which will be enhanced with increasing hybridization. This finding seems to be consistently correlated with thermodynamic properties of XMnSb (X = Pt, Ni) [1], considering that T_C of NiMnSb (~ 730 °C) is much larger than that of PtMnSb (~ 580 °C). The overall thermodynamic properties of PtMnSb and PdMnSb are similar, while they are very different from those of NiMnSb [1, 2]. This is again consistent with the findings in this study: (i) that the experimental Mn 3d PSW of PtMnSb and PdMnSb are similar, and (ii) that the calculated X d PLDOS of XMnSb with X = Pt is rather similar to that with X = Pd but different to that with X = Ni.

3.2. Sb 4d core level photoemission

We now discuss the Sb 4d core level spectra of XMnSb (X = Pt, Pd, Ni) by comparing the data taken at $h\nu$ = 72 eV in figure 7. For X = Pt and Ni, two main peaks at higher BE correspond to the spin–orbit split *bulk* Sb $4d_{5/2}$ (~ 32 eV) and $4d_{3/2}$ (~ 33.2 eV) components, and two shoulders at lower BE (~ 31.5 eV and ~ 32.7 eV) arise from *surface*-shifted Sb $4d_{5/2}$ and $4d_{3/2}$ emissions. This identification has been supported by the observation that, when more *bulk*-sensitive $h\nu$ were used for incident photons or when the sample surfaces were intentionally contaminated, the lower BE peaks decreased as compared with the higher BE peaks.

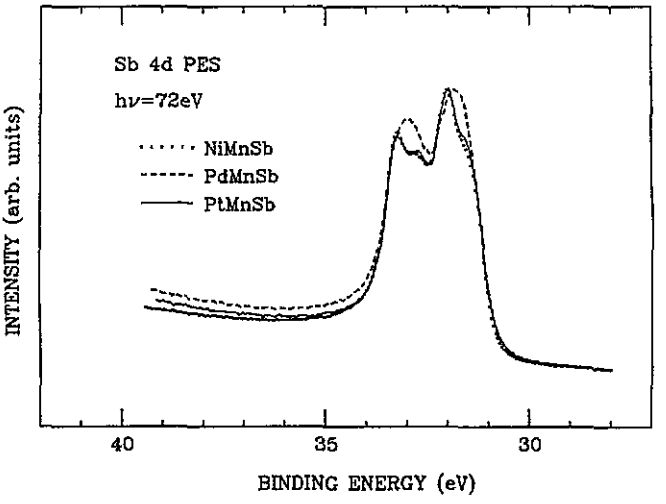

Figure 7. Comparison of the Sb 4d core level PES spectra of XMnSb (X = Pt, Pd, Ni), taken at $h\nu$ = 72 eV. Two peaks correspond to the spin–orbit split Sb $4d_{5/2}$ and $4d_{3/2}$ components.

Note that the Sb 4d core level spectrum of PtMnSb is essentially identical to that of NiMnSb, but that the Sb 4d peaks in PdMnSb are broader with less structures than those in PtMnSb and NiMnSb. The larger linewidth in the Sb 4d spectra might be attributed to several factors: (i) different atomic arrangements due to segregation or irregular cleavage plane at the surface†, which will lead to inhomogeneous *surface*-shifted emissions with respect to *bulk* emissions, (ii) inhomogeneity of the sample due to the presence of grain boundaries, (iii) a shorter lifetime of the Sb 4d core hole due to Auger recombination [29], or (iv) larger hybridization between Sb 5s/5p and other valence electrons. The second mechanism is refuted, as checked by XRD and SEM analyses (see section 2).

To find which factors cause the differences observed in the Sb 4d core level PES line shapes of XMnSb (X = Pt, Pd, Ni), we have performed a curve-fitting analysis of the Sb 4d PES spectra. Each peak is fitted with a Doniach–Sùnjic line shape [30, 31] by adjusting two parameters: the FWHM of the Lorentzian function 2γ and the asymmetry factor α. The physical meanings of these parameters are to incorporate the effect of the finite lifetime of the core hole state and the effect of the many-body line shape due to the electron–hole pairs, respectively. The peaks are further convoluted with a Gaussian of 0.23 eV at FWHM to account for the instrumental resolution. For all three X, a value of 2.1 eV is used for the spin–orbit splitting between Sb $4d_{5/2}$ and $4d_{3/2}$ components, and 2/3 is used for the intensity ratio of the Sb $4d_{3/2}$ peak to the $4d_{5/2}$ peak. Finally, a background is added to account for the inelastically scattered electrons, by assuming that the amount of the background is proportional to the total integrated intensity at higher kinetic energies.

The results of curve fittings for NiMnSb and PdMnSb are presented in figures 8(*a*) and (*b*), respectively‡. The parameters, obtained from the curve fitting, are summarized in table 1. One can see two noticeable differences between X = Pd and X = Ni, Pt. First, the linewidth parameter for PdMnSb ($2\gamma \sim 0.80$) is larger than those for NiMnSb and PtMnSb ($2\gamma = 0.48 \sim 0.60$). Second, the surface core level shift Δ_{SCS} for PdMnSb (0.33 eV) is smaller than for NiMnSb or PtMnSb (0.50 eV). These differences are surprising since the Sb 4d spectrum should be influenced most dominantly by the Sb 5s/5p electrons via intra-atomic Auger processes, which are expected to be insensitive to X atoms because of their delocalized nature. One explanation for the origin of a larger 2γ for X = Pd might be that the metallic character of the minority-spin states in PdMnSb [16] leads to a larger probability in inter-atomic Auger recombination compared with the insulating minority-spin states in PtMnSb and NiMnSb. A larger Auger recombination for X = Pd will cause a shorter Sb 4d core hole lifetime and a larger value in 2γ, than for X = Pt and Ni. Similarly, the metallic character of the minority-spin states in PdMnSb would yield a better screening for a core hole final state, and so a smaller value of Δ_{SCS}, as compared to the insulating minority-spin states in PtMnSb and NiMnSb [16].

There are other minor differences in the fitting parameters. The asymmetry factor for PdMnSb ($\alpha = 0.11$) is slightly larger than that for NiMnSb or PtMnSb ($\alpha = 0.08$), and the intensity ratio of the *surface* to *bulk* emission I_S/I_B for PdMnSb ($I_S/I_B = 1.1$) is also slightly larger than that for NiMnSb or PtMnSb ($I_S/I_B = 1.0$). These differences might suggest a larger metallic character and a larger *surface* contribution for X = Pd than for X = Ni and Pt. However, the magnitudes of these differences are within the uncertainty of the fitting parameters.

† Note that all three samples were polycrystalline. Their cleaved surfaces were rather rough, suggesting irregular cleavage planes for all three samples. Valence band spectra (see figure 1 and [13]) and core level XPS spectra [14] of XMnSb show that the sample quality of PdMnSb is at least as good as those of PtMnSb and NiMnSb. The samples in this work are the same ones used in the XPS measurements described in [14].

‡ Since the results for PtMnSb are essentially identical to those for NiMnSb, they are not presented in this paper.

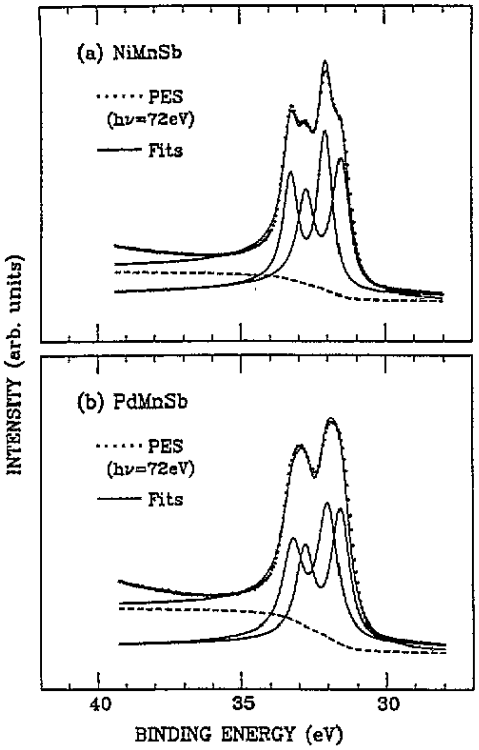

Figure 8. (*a*) Curve fitting results (full curves) of Sb 4d core levels, in comparison with the measured PES spectra (dots) for NiMnSb. Broken curves represent a background, added to the fits, to account for the inelastically scattered electrons. (*b*) Same for PdMnSb.

Table 1. Fitting parameters for the Sb 4d core level PES spectra shown in figure 8. The terms $2\gamma_B$ and $2\gamma_S$ correspond to the FWHM of the Lorentzian broadening of the *bulk* and *surface* components, respectively; α denotes the asymmetry factor; Δ_{SCS} denotes the surface core level shift, i.e. the separation between *surface* and *bulk* components; I_S/I_B represents the *surface*-to-*bulk* intensity ratio.

	$2\gamma_B$	$2\gamma_S$	α	Δ_{SCS}	I_S/I_B
NiMnSb (PtMnSb)	0.52	0.60	0.08	0.50	1.0
PdMnSb	0.80	0.80	0.11	0.33	1.1

4. Conclusions

The electronic structure of the Heusler alloys XMnSb (X = Pt, Pd, Ni) have been investigated using photoemission spectroscopy. The PSW distributions of Mn 3d and X d valence electrons have been determined and compared with the calculated PLDOS. The experimental Mn 3d PSW of PtMnSb and PdMnSb are found to be almost identical. They extend over the entire valence band, suggesting large hybridization between Mn 3d and other valence electrons. Furthermore, they are quite different from that of Mn metal, but are analogous to that of MnO, indicating that the role of the Sb 5p electrons in determining the electronic and magnetic structures of the Mn 3d states in XMnSb (X = Pt, Pd) might

be similar to that of the O 2p electrons in MnO.

In the comparison between experimental PSW and theoretical PLDOS, fairly good agreement is observed for the Pt and Pd d states, whereas large discrepancies are observed for the Mn 3d states. NiMnSb exhibits large disagreement between the experimental PES spectrum and the weighted sum of the Mn and Ni 3d PLDOS, such as peak positions, band widths and spectral weight near E_F. These discrepancies seem to arise from the large Mn and Ni 3d Coulomb correlation interactions. The calculated X d and Mn 3d PLDOS shows that the hybridization between the Mn 3d and X d states increases as X varies from X = Pt to Pd and Ni. This finding is consistently correlated with thermodynamic properties of XMnSb (X = Pt, Ni) in that the T_C of NiMnSb is much larger than that of PtMnSb.

The measured Sb 4d core level spectrum of XMnSb with X = Pd shows a broader linewidth with less structures than those with X = Pt, Ni. The line shape analysis of the Sb 4d PES spectra indicates that the major differences in the fitting parameters are a larger lifetime broadening and a smaller *surface* core level shift in PdMnSb than in PtMnSb and NiMnSb. These differences are consistent with the metallic character of the minority-spin states in PdMnSb, in contrast to the insulating character of the minority-spin states in PtMnSb and NiMnSb.

Acknowledgments

This work has been supported by the POSTECH-BSRI program of the Korean Ministry of Education. The travel fund for the synchrotron experiments was provided by the Pohang Light Source. The Synchrotron Radiation Center is supported by the US National Science Foundation.

References

[1] van Engen P G, Buschow K H J, Jongebreur R and Erman M 1983 *Appl. Phys. Lett.* **42** 202
[2] de Groot R A, Mueller F M, van Engen P G and Buschow K H J 1983 *Phys. Rev. Lett.* **50** 2024
[3] Wijngaad J H, Haas C and de Groot R A 1989 *Phys. Rev.* B **40** 9318
[4] de Groot R A, Mueller F M, van Engen P G and Buschow K H J 1984 *J. Appl. Phys.* **55** 2151
[5] Kulatov E and Mazin I I 1990 *J. Phys.: Condens. Matter* **2** 343
[6] Kübler J, Williams A R and Sommers C B 1983 *Phys. Rev.* B **28** 1745
[7] Youn S J and Min B I 1995 *Phys. Rev.* B **51** to appear
[8] Takanashi K, Watanabe J, Kido G and Fujinori H 1990 *Japan. J. Appl. Phys.* **29** L306
[9] Kamper K P, Schmitt W, Güntherodt G, Gambino R J and Ruf R 1987 *Phys. Rev. Lett.* **59** 2788
[10] Bona G L, Meier F, Taborelli M, Bucher E and Schmidt P H 1985 *Solid State Commun.* **56** 391
[11] Kisker E, Carbone C, Flipse C F and Wassermann E F 1987 *J. Magn. Magn. Mater.* **70** 21
[12] Robey S W, Hudson L T and Kurtz R L 1992 *Phys. Rev.* B **46** 11 697
[13] Kang J-S, Hong J H, Jung S W, Lee Y P, Park J-G, Olson C G, Youn S J and Min B I 1993 *Solid State Commun.* **88** 653
[14] Yang S-H, Oh S-J and Park J-G 1994 unpublished
Yang S-H 1994 *MSc Thesis* Seoul National University
[15] Helmholdt R B, de Groot R A, Müller F M, van Engen P G and Buschow K H J 1984 *J. Magn. Magn. Mater.* **43** 249
[16] Min B I unpublished
[17] Taylor A and Kagle B J (ed) 1963 *Crystallographic Data on Metal and Alloy Structures* (New York: Dover)
[18] Andersen O K 1975 *Phys. Rev.* B **12** 3060
Skriver H L 1984 *The LMTO Method (Springer Series in Solid State Sciences 41)* (Berlin: Springer)
[19] Hohenberg P and Kohn W 1964 *Phys. Rev.* **136** B864
Kohn W and Sham L J 1965 *Phys. Rev.* **140** A1133

[20] Cooper J W 1962 *Phys. Rev.* **128** 681
Fano U and Cooper J W 1968 *Rev. Mod. Phys.* **40** 441
Bancroft G M, Gudat W and Eastman D E 1978 *Phys. Rev.* B **17** 4499
Abbati I, Braicovich L, Rossi G, Lindau I, del Pennino U and Nannarone S 1983 *Phys. Rev. Lett.* **50** 1799
[21] Scofield J H 1976 *J. Electron Spectrosc. Rel. Phenom.* **8** 129
Yeh J J and Lindau I 1985 *At. Data Nucl. Data Tables* **32** 1
[22] Shirley D A 1972 *Phys. Rev.* B **5** 4709
[23] Sugawara H, Kakizaki A, Nagakura I and Ishii T 1982 *J. Phys. F: Met. Phys.* **12** 2929
[24] Raaen S and Murgai V 1987 *Phys. Rev.* B **36** 887
[25] Eastman D E and Freeouf J L 1975 *Phys. Rev. Lett.* **34** 395
[26] Naito K, Kakizaki A, Komatsubara T, Sugawara H, Nagakura I and Ishii T 1985 *J. Phys. Soc. Japan* **54** 416
[27] Lad R J and Henrich V E 1988 *Phys. Rev.* B **38** 10 860
[28] Ashcroft A W and Mermin N D 1976 *Solid State Physics* (New York: Holt, Rinehart and Winston)
[29] Mahan G D 1986 *Many-Particle Physics* (New York: Plenum) p 746
[30] Doniach S and Sùnjic M 1970 *J. Phys. C: Solid State Phys.* **3** 285
[31] Wertheim G K and Citrin P H 1978 *Photoemission in Solids I* ed M Cardona and L Ley (Berlin: Springer) p 197